# 1
# The Isotopic Composition of the Elements

*Frank Vanhaecke and Kurt Kyser*

## 1.1
## Atomic Structure

Early in the twentieth century, Rutherford realized that Thomson's late nineteenth century plain cake model for the atom, describing the atom as consisting of electrons floating around in a positive sphere, had to be replaced by a "Saturnian" model, describing the atom as consisting of a small central nucleus surrounded by electrons, rotating on rings [1]. This view was supported by a study of the behavior of a beam of α particles (see below, particles resembling the nucleus of an He atom, thus consisting of two protons and two neutrons) directed on to a very thin Au metal foil, known as the Geiger–Marsden experiment [2]. Since only a minor fraction of the α-particles were recoiled or deflected, and for the majority the path was not affected, it had to be concluded that for the largest part, an atom consists of empty space. According to Bohr's later model [3], the atom contains a nucleus composed of positively charged protons and neutral neutrons, having approximately the same mass. This nucleus is a factor of $\sim 10^4$ smaller than the size of the atom (although the concept of size itself is not self-evident in this context) and holds practically all of its mass. As they both reside in the nucleus, protons and neutrons are also referred to by the common term nucleon. The negatively charged electrons are substantially lighter (almost 2000 times) and rotate around the central nucleus in different orbits (also termed shells), corresponding to different energy levels. Subsequently, insight into the atomic structure has evolved tremendously and a multitude of other particles have been discovered, but for many chemical considerations – including a discussion of isotopes – the Bohr model still largely suffices.

As all protons carry the positive unit charge ($1.602 \times 10^{-19}$ C), they mutually repel one another. This electrostatic repulsion is overcome by the so-called nuclear force [4]. This is a very strong force, but effective only within a very short range. In fact, the very short range over which this force is effective even causes the largest nuclei (e.g., those of U) to be unstable (see below). Further clarification of the nature of this nuclear force requires a more thorough discussion of the atomic

*Isotopic Analysis: Fundamentals and Applications Using ICP-MS*,
First Edition. Edited by Frank Vanhaecke and Patrick Degryse.

Published 2012 by WILEY-VCH Verlag GmbH & Co. KGaA

structure, including a discussion on quarks, but this is beyond the scope of this chapter. Electrostatic attraction between the positive nucleus and the orbiting negative electrons provides the centripetal force required to keep the electrons from drifting away from the nucleus.

## 1.2 Isotopes

The chemical behavior of an atom is governed by its valence electrons (electron cloud) and, therefore, atoms that differ from one another only in their number of neutrons in the nucleus display the same chemical behavior (although this statement will be refined later). Such atoms are called isotopes and are denoted by the same chemical symbol. The term isotopes refers to the fact that different nuclides occupy the same position in the periodic table of the elements and was introduced by Todd and Soddy in the early twentieth century [5].

To distinguish between the isotopes of an element, the mass number $A$ – corresponding to the sum of the number of protons and the number of neutrons (the number of nucleons) in the nucleus – is noted as a superscript preceding the element symbol: ${}^{A}\mathrm{X}$. The atomic number $Z$, corresponding to the number of protons in the nucleus, may be added as a subscript preceding the element symbol $-{}^{A}_{Z}\mathrm{X}$ – but is often omitted as this information is already inherent in the element symbol.

As a result of their difference in mass, isotopes of an element can be separated from one another using mass spectrometry (MS), provided that they are converted into ions. In fact, this is exactly how isotopes were discovered: Thomson separated the ion beams of two Ne isotopes using a magnetic field, while their detection was accomplished with a photographic plate [6]. With a similar setup, typically referred to as a mass spectrograph, Aston was subsequently able to demonstrate the existence of isotopes for a suite of elements [7].

Although several techniques provide a different response for the isotopes of an element, for example, infrared (IR) spectroscopy, nuclear magnetic resonance (NMR) spectroscopy and neutron activation analysis (NAA), MS is the technique of choice for the majority of isotope ratio applications. The isotopic composition of the light elements H, C, N, O, and S is typically studied via gas source MS, and for $^{14}\mathrm{C}$ dating, accelerator mass spectrometry (AMS) is replacing radiometric techniques to an increasing extent. For isotopic analysis of metals and metalloids, thermal ionization mass spectrometry (TIMS) and inductively coupled plasma mass spectrometry (ICP-MS) are the methods of choice. This book is devoted to the use of (single-collector and multi-collector) ICP-MS in this context and its basic operating principles, capabilities, and limitations are discussed in Chapters 2 and 3.

The relative abundance of one nuclide of the element M ($^{1}\mathrm{M}$) is calculated as the amount (number of atoms $N$ or number of moles $n$) of nuclide $^{1}\mathrm{M}$ divided by the total amount (number of atoms or number of moles) of the element M:

$$\theta(^1\mathrm{M}) = \frac{N(^1\mathrm{M})}{\sum_{i=1}^{i=m} N(^i\mathrm{M})} = \frac{n(^1\mathrm{M})}{\sum_{i=1}^{i=m} n(^i\mathrm{M})}$$

for an element with $m$ isotopes.

## 1.3 Relation Between Atomic Structure and Natural Abundance of Elements and Isotopes

Except for the lightest atoms, the binding energy per nucleon is remarkably stable (varying only from 7.6 to 8.8 MeV) for the naturally occurring elements (Figure 1.1). On the basis of this curve, it is understood that fission of a heavy nucleus

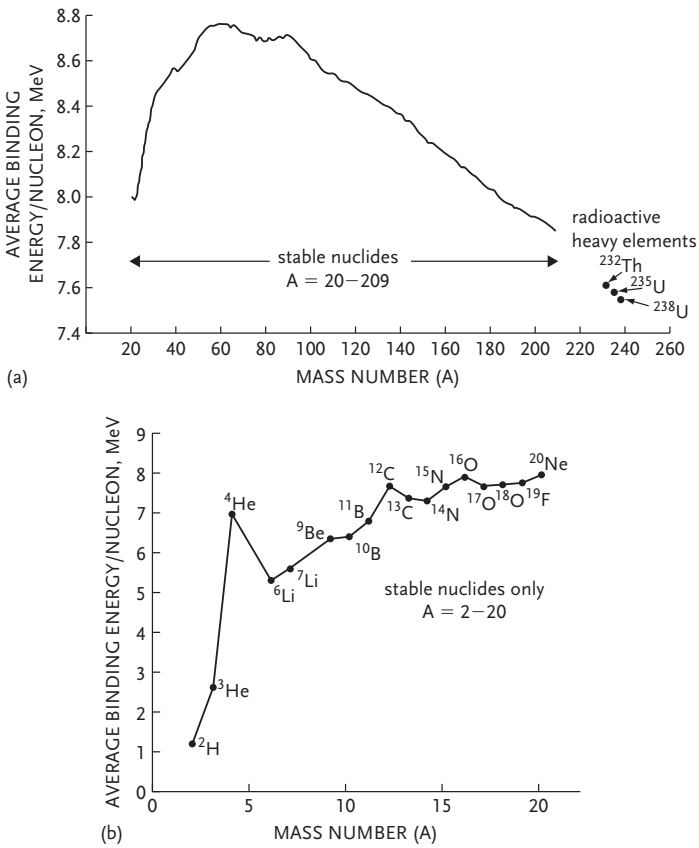


**Figure 1.1** (a) Average binding energy per nucleon as a function of mass number for nuclides with a mass number from 20 to 238. (b) Average binding energy per nucleon as a function of mass number for nuclides with a mass number from 1 to 20. Reproduced with permission of John Wiley & Sons, Ltd., from [8].

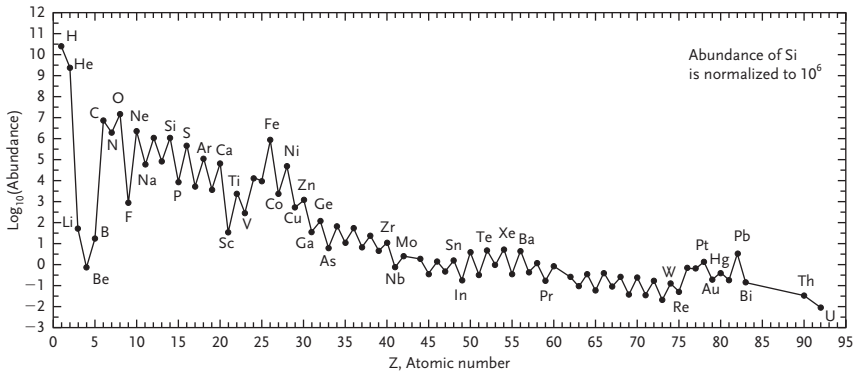


**Figure 1.2** Natural relative abundance of the elements as a function of their atomic number. Reproduced with permission of John Wiley & Sons, Ltd., from [9]. The graph is based on the data published by Lodders [10].

into lighter nuclei (e.g., in a nuclear reactor) or fusion of two H atoms into He (the basis of solar energy) are exo-energetic because the process results in nuclei/a nucleus characterized by a substantially higher binding energy per nucleon.

With the lighter atoms (see Figure 1.1b), nuclei with an even number of protons and an even number of protons show a higher binding energy per nucleon and thus higher stability (compare, e.g., the binding energies for $^{4}$He and $^{3}$He, $^{12}$C and $^{13}$C, and $^{16}$O and $^{17}$O). In addition, elements with an even number of protons, reflected by an even atomic number $Z$, are more abundant in Nature than those with an uneven number (Figure 1.2).

This variation in binding energy per nucleon also exerts a pronounced effect on the isotopic composition of the elements, especially for the light elements. "Even–even isotopes" for elements such as C and O ($^{12}$C and $^{16}$O) are much more abundant than their counterparts with an uneven number of neutrons ($^{13}$C and $^{17}$O). Despite the *overall* limited variation in binding energy per nucleon as a function of the mass number for the heavier elements, its variation among isotopes of an element may vary substantially, leading to a preferred occurrence of even–even isotopes, as illustrated by the corresponding relative isotopic abundances for elements such as Cd and Sn (Table 1.1). In both the lower ($^{106}$Cd through $^{110}$Cd) and the higher ($^{114}$Cd through $^{116}$Cd) mass ranges, only Cd isotopes with an even mass number occur. In addition, the natural relative isotopic abundances for $^{113}$Cd and, to a lesser extent, $^{111}$Cd are low in comparison with those of the neighboring Cd isotopes with an even mass number. Similarly, Sn, for which 7 out of its 10 isotopes are characterized by an even mass number, the isotopes with an odd mass number have a lower natural relative abundance than their neighbors.

**Table 1.1** Isotopic composition of Cd and Sn according to Böhlke *et al*. [11].

| Element | Atomic number $Z$ | Isotopes and natural relative abundances (mol%) | |
|---|---|---|---|
| Cd | 48 | $^{106}$Cd | 1.25 |
| | | $^{108}$Cd | 0.89 |
| | | $^{110}$Cd | 12.49 |
| | | $^{111}$Cd | 12.80 |
| | | $^{112}$Cd | 24.13 |
| | | $^{113}$Cd | 12.22 |
| | | $^{114}$Cd | 28.73 |
| | | $^{116}$Cd | 7.49 |
| Sn | 50 | $^{112}$Sn | 0.97 |
| | | $^{114}$Sn | 0.66 |
| | | $^{115}$Sn | 0.34 |
| | | $^{116}$Sn | 14.54 |
| | | $^{117}$Sn | 7.68 |
| | | $^{118}$Sn | 24.22 |
| | | $^{119}$Sn | 8.59 |
| | | $^{120}$Sn | 32.58 |
| | | $^{122}$Sn | 4.63 |
| | | $^{124}$Sn | 5.79 |

## 1.4 Natural Isotopic Composition of the Elements

As a first approximation, it can be stated that all elements have an isotopic composition that is invariant in Nature. This is the result of thorough mixing of most nuclides prior to the formation of the solar system some 4.6 billion years ago [12]. Addition of a stable isotopic tracer to a natural system induces a change in the isotopic composition of a target element. The use of isotope dilution for elemental assay (Chapter 8) and tracer experiments for monitoring a physical or a (bio)chemical process (Chapter 16) are based on measuring the induced changes in the isotopic composition of a target element thus obtained, as discussed in later chapters.

There are, however, various reasons why elements may show variations in their natural isotopic composition:

- **Radiogenic nuclides:** Some elements have one or several radiogenic nuclides, meaning that over time, such a nuclide is being produced as a result of the decay of a naturally occurring and long-lived radionuclide. The additional production of such a radiogenic nuclide has a pronounced effect on the temporal isotopic composition of the element with (the) radiogenic nuclide(s)

and – as a result of the way in which isotopic abundances are defined – also affects the relative isotopic abundances of the other isotopes.

- **Extraterrestrial materials:** In some extraterrestrial material such as meteorites, elements may show isotopic compositions that are distinct from all terrestrial material investigated. This is related to decay of radionuclides that may already be extinct, due to half-lives which are very short compared with the age of the solar system of $4.6 \times 10^9$ years. Such variations are rare for terrestrial materials, in large part due to preferential sampling of the crust, whereas some extraterrestrial material, such as iron meteorites, resemble the Earth's core, in which parent to daughter element ratios may be much higher than in the crust.
- **Interaction between cosmic rays and terrestrial matter:** The Earth's atmosphere and, to a lesser extent, its surface are constantly bombarded with cosmic radiation which interacts with terrestrial material, resulting in isotopic variations in some elements. The best known example is the production of $^{14}C$ from $^{14}N$ by (n,p) reaction in the atmosphere, with the neutron involved created by cosmic ray-induced spallation. $^{14}C$, a radionuclide with a half-life of 5730 years, is oxidized to $CO_2$ and enters the food chain via photosynthesis, thus affecting the isotopic composition of C in all living organisms.
- **Mass-dependent isotope fractionation:** The original theory that isotopes of an element are chemically identical has to be refined. As a result of their slight difference in mass, the isotopes of an element tend to participate in physical processes and (bio)chemical reactions with slightly different efficiencies. These differences in efficiency are related to a slight difference in equilibrium for each different isotopic molecule (thermodynamic effect) or in the rate with which the isotopes participate in a process or reaction (kinetic effect). This phenomenon is referred to as isotope fractionation and is well characterized for the lighter elements H, C, N, O, and S, the isotopic composition of which is typically studied via gas source isotope ratio MS. Especially the light elements that are redox sensitive show substantial variations in their isotopic composition, because different oxidation states correspond to substantially different bonding environments. In general, the extent of isotope fractionation is governed by the extent to which an element takes part in physical processes, such as diffusion, or chemical reactions wherein there is a change in bonding environment, and the relative difference in mass between the isotopes. Among the metals and metalloids, Li and B show significant natural isotopic variations as a result of isotope fractionation because of the large relative difference in mass of their isotopes. For the heavier elements – for which the isotopes show a much smaller relative mass difference – conventional wisdom held that there was minimal isotope fractionation, but the enhanced capabilities offered by state-of-art MS have demonstrated that all elements are prone to isotope fractionation, even an element as heavy as U [13].
- **Mass-independent fractionation:** Most cases of isotope fractionation are characterized by a linear relationship between the magnitude of the effect established and the difference in mass between the isotopes considered. For an increasing number of elements, however, an apparently aberrant behavior is established for some of their isotopes. This is currently a hot topic of research

and is attributed to a subtle difference in the interaction between the nucleus of those isotopes and the surrounding electron cloud, which affects the bonding environment for certain isotopes and results in mass-independent fractionation of these nuclides in chemical reactions. The interaction between the nucleus and the electron cloud in such instances is hypothesized to be influenced by variation in the volume of the nucleus or in its magnetic properties (see below). Mass-independent fractionation provides the elements with a distinct isotopic pattern that differs from that predicted by mass-dependent fractionation processes.

- **Anthropogenic effects:** Via a variety of processes, human-made changes in the isotopic composition of an element can be accomplished by enhancing the fractionation beyond those in normal reactions, or by producing specific isotopes. Production of enriched U for fueling nuclear reactors and production of enriched isotopic tracers for tracer experiments or for isotope dilution MS are examples of the effects of human intervention on isotopic compositions.

Various processes that result in isotopic variations will be discussed in more detail in the following sections. The way in which the quantification of such variations can be used in the context of various real-life applications will be demonstrated in later chapters.

### 1.4.1
### Elements with Radiogenic Nuclides

#### 1.4.1.1 Radioactive Decay

When considering all nuclides that occur in Nature, a distinction can be made between stable and radioactive nuclides (radionuclides). The nucleus of a radionuclide undergoes spontaneous radioactive decay, whereby it is converted into another nucleus.

Several types of radioactive decay can occur [4, 8, 14].

In the case of α-decay, an α-particle, containing two protons and two neutrons, is emitted from the nucleus, resulting in a reduction in its mass number by four units and in its atomic number by two mass units:

$$^{A}_{Z}\mathrm{X} \rightarrow {}^{A-4}_{Z-2}\mathrm{Y} + {}^{4}_{2}\alpha$$

α-Decay predominantly occurs for very heavy nuclides with an atomic mass number $>200$.

The term β-decay is used for those decay processes in which the mass number of the decaying nuclide remains the same, but the atomic number changes. This situation occurs in case of conversion of:

- a neutron into a proton, accompanied by emission of a $\beta^-$ particle (i.e., an electron emitted by the nucleus, also called a negatron)
- a proton into a neutron, caused by the capture of an electron, usually coming from the K shell, or accompanied by emission of a $\beta^+$ particle (also called a positron).

Nuclides with a relative excess of neutrons are prone to $\beta^-$-decay, nuclides with a relative excess of protons (or shortage of neutrons) to $\beta^+$-decay.

Whereas α-particles are characterized by specific energies, the energies of emitted β-particles show a continuous distribution. This puzzled scientists for a long time, but was understood when it was realized that β-decay is accompanied by the emission of a neutrino or anti-neutrino and the energy that is released is distributed over the β-particle and the (anti)neutrino. Hence the various forms of β-decay can be described as follows:

$$\begin{aligned}
&\beta^- \text{ decay}: && {}^{A}_{Z}\mathrm{X} \rightarrow {}^{A}_{Z+1}\mathrm{Y} + {}^{0}_{-1}\beta^- + \overline{\nu}\\
&\beta^+ \text{ decay}: && {}^{A}_{Z}\mathrm{X} \rightarrow {}^{A}_{Z-1}\mathrm{Y} + {}^{0}_{1}\beta^+ + \nu\\
&\text{electron capture}: && {}^{A}_{Z}\mathrm{X} + {}^{0}_{-1}\mathrm{e}^- \rightarrow {}^{A}_{Z-1}\mathrm{Y} + \nu
\end{aligned}$$

In addition, when a nucleus is in an excited state, it can emit γ-radiation. In this case, the difference in energy between the higher and the lower energy states is emitted in the form of a γ-photon upon relaxation. Emission of this radiation does not affect either the atomic number or the mass number.

A nuclide can undergo spontaneous radioactive decay when the process is energetically favorable, which necessitates the sum of the masses of the resulting particles being smaller than the sum of the masses of the starting particles in all instances, except electron capture.

The radioactive decay process is normally a first-order reaction with a characteristic half-life $T_{1/2}$ – this is the time interval in which half of the nuclide population decays – and corresponding decay constant λ:

$$\lambda = \frac{\ln 2}{T_{\frac{1}{2}}}$$

As a result of this first-order behavior, radioactive decay is a process that can be described mathematically by an exponential decrease in the number of parent nuclides $N$ as a function of time (Figure 1.3):

$$N_t = N_0 \mathrm{e}^{-\lambda t}$$

where $N_t$ is the number of parent nuclides at time $t$ and $N_0$ is the original number of nuclides at time = 0.

Therefore, this phenomenon can be exploited for dating processes. Among the most widespread dating methods is radiocarbon dating, relying on the $\beta^-$ decay of $^{14}$C, which allows for age determination of the remains of living organisms (time passed since time of death), such as human remains or wood [15]. Because radiocarbon dating involves either radiometry or AMS, it will not be covered in this book. Other dating methods, such as U, Th–Pb, Pb–Pb, and Rb–Sr dating, however, can be carried out, relying on isotope ratio measurements via ICP-MS, and are discussed in detail in Chapter 9.

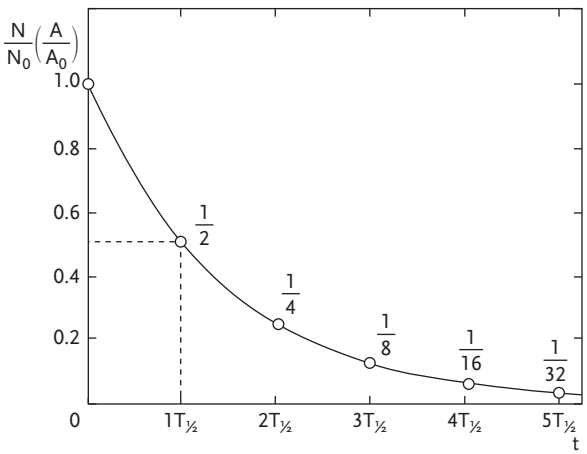


**Figure 1.3** Decrease in the number of parent nuclides as a function of time *t* as a result of radioactive decay.
Reproduced with permission of Ellis Horwood from [14].

#### 1.4.1.2 Elements with Radiogenic Nuclides

Some elements show natural variations in their isotopic composition because one or more of their isotopes are radiogenic [9, 16]. A radiogenic nuclide is continuously produced by decay of a naturally occurring radionuclide, thus leading to a steadily increasing relative abundance of this isotope, at least as long as the parent radionuclide and daughter radiogenic nuclide reside together. Because of the way in which relative isotopic abundances are calculated, the presence of one radiogenic nuclide affects the relative abundance of all isotopes of the daughter element.

The natural variation observed for elements with radiogenic isotopes is fairly pronounced and their isotopic analysis can serve various purposes. Once the half-life of the parent nuclide is known, then is its decay rate and thus the generation rate of the daughter (or progeny) nuclide and isotopic analysis can be used for dating (age determination) purposes, as described in Chapter 9. In addition to the geochronological application, isotopic analysis of these elements can also be used for provenance determination, that is, determination of the (geographic) origin of a material, object, or living species, as is discussed in detail in later chapters.

Examples of elements showing radiogenic isotope accessible via ICP-MS are provided below.

**Strontium** Strontium has four stable isotopes ($^{84}$Sr, $^{86}$Sr, $^{87}$Sr, and $^{88}$Sr), one of which, $^{87}$Sr, is radiogenic, as it is produced via the $\beta^-$ decay of $^{87}$Rb:

$$^{87}\mathrm{Rb} \rightarrow {}^{87}\mathrm{Sr} + \beta^- + \overline{\nu}$$

where $\beta^-$ represents the particle emitted from the $^{87}$Rb nucleus and $\overline{\nu}$ an anti-neutrino. The corresponding half-life is $48.8 \times 10^9$ years, which is more than 10

times the age of the solar system, such that only a limited fraction of $^{87}$Rb has decayed so far.

Although the isotopic composition of Rb, which has two isotopes, $^{85}$Rb and $^{87}$Rb, varies slowly as a function of time, no fractionation of Rb isotopes is known to occur so that the isotopic composition of Rb currently is the same for all terrestrial material. In contrast, the isotopic composition of Sr does show natural variation as a result of the decay of $^{87}$Rb and between rocks or minerals the isotopic composition of Sr will vary, depending on their Rb/Sr ratio and the time during which these elements have spent together. As the Rb/Sr elemental ratio and the Sr isotopic composition or, more specifically, the ratio of the radiogenic nuclide to a reference isotope, typically $^{87}$Sr/$^{86}$Sr, are measurable, this decay can be used for geochronological purposes (see Chapter 9). In addition, Sr isotopic analysis is also deployed in the context of the determination of the provenance of, among other things, agricultural products and human remains (in an archaeological or forensic context) and for providing insight into human and animal migration behavior [17] (see Chapters 13 and 14).

**Lead** Lead has four stable isotopes, three of which are radiogenic. The decay chains of $^{238}$U ($T_{1/2} = 4.468 \times 10^9$ years), $^{235}$U ($T_{1/2} = 0.407 \times 10^9$ years), and $^{232}$Th ($T_{1/2} = 14.010 \times 10^9$ years) finally result in $^{206}$Pb, $^{207}$Pb, and $^{208}$Pb as daughters, respectively (Figure 1.4), and only $^{204}$Pb is not radiogenic.

For all three decay chains, the first step is much slower than the subsequent steps and, for many practical purposes, the entire chain can be described as a one-step process. As a result of these processes, the isotopic composition of Pb is governed by the U/Pb and Th/Pb elemental ratios and the times during which these elements have resided together. There is a substantial difference between the isotopic composition of crustal Pb and that in ores, because upon ore formation Pb was separated from U and Th and its isotopic composition was therefore "frozen" at that moment, while in the Earth's crust the decay of the parents continued to affect the isotopic composition of Pb. As a result, Pb isotopic analysis provides an excellent tool to distinguish between local (crustal) Pb and Pb pollution resulting from ore-derived Pb (e.g., used in anti-knock compounds previously added to petrol or used for other industrial purposes) [19–25]. Pb ores also show different isotopic signatures among them and therefore, Pb isotopic analysis is also widely deployed as a means of provenance determination of objects of art [17] or of tracing transport of dust [22, 23, 26].

For environmental samples, such as atmospheric aerosols, sediments, and snow, Pb from several sources may contribute to the total Pb concentration and therefore the isotopic signature will be a mixture of those of the various contributions. When there is mixing between Pb from two sources, the Pb isotope ratio results plotted on a three-isotope plot, that is, one isotope ratio of Pb, plotted as a function of another with a common denominator (Figure 1.5), will fall on a straight mixing line between the two end-member compositions, and the extent to which each of the two sources contributes to the sample's signature can be calculated [27]. If one Pb isotope ratio is plotted as a function of the Pb

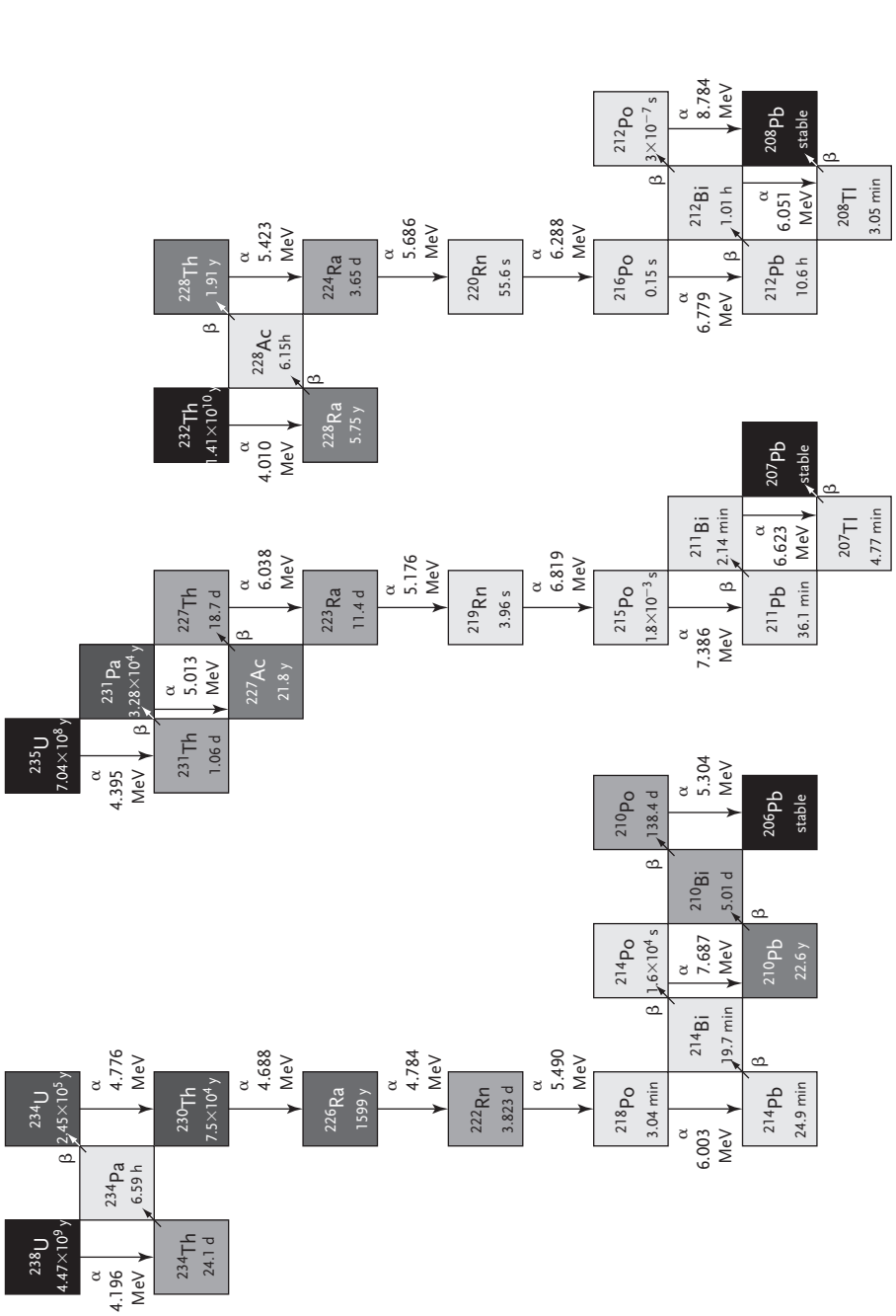


**Figure 1.4** Decay of the naturally occurring and long-lived radionuclides $^{238}U$, $^{235}U$, and $^{232}Th$, with $^{206}Pb$, $^{207}Pb$, and $^{208}Pb$ as stable end products, respectively. The gray scale of the nuclides in the decay chains gives an indication of the corresponding half-lives, with darker gray for longer values. Reproduced with permission of the Mineralogical Society of America – Geochemical Society from [18].

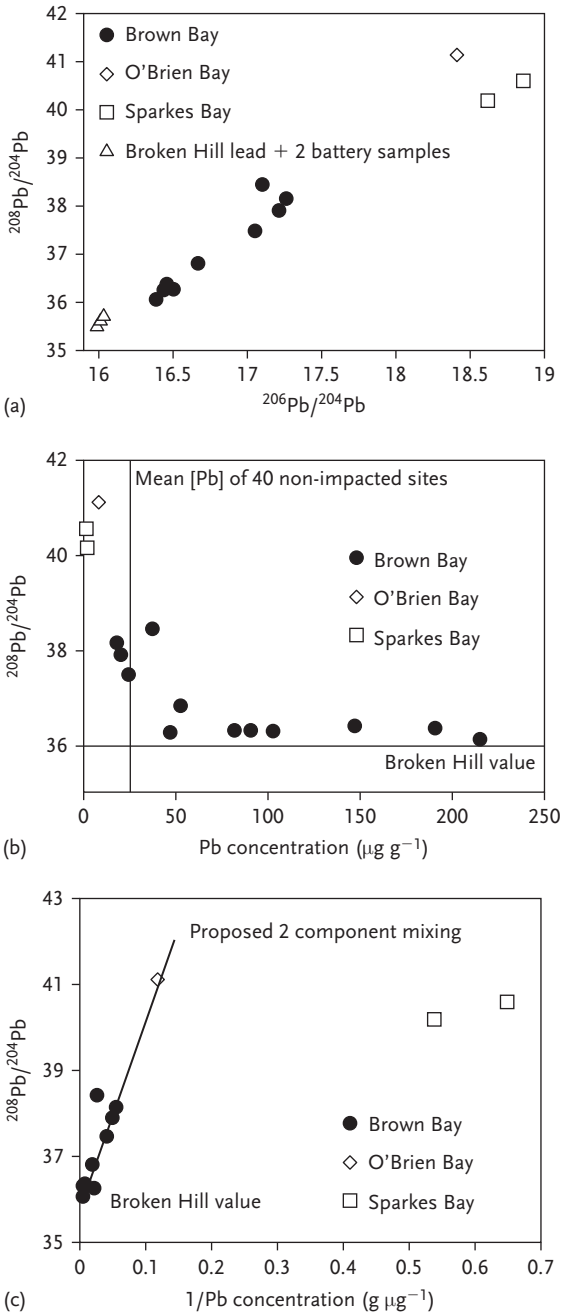


**Figure 1.5** Three-isotope plot ($^{208}Pb/^{204}Pb$ versus $^{206}Pb/^{204}Pb$) for Antarctic sediments from the Pb-polluted Brown Bay (filled circles) and proxies for potential Pb sources – Broken Hill Pb ore and battery samples for anthropogenic Pb, on the one hand, and unpolluted sediments for local crustal Pb, on the other (O'Brien Bay and Sparkes Bay). (b) $^{208}Pb/^{204}Pb$ versus Pb concentration. (c) $^{208}Pb/^{204}Pb$ versus 1/Pb concentration.
Reproduced with permission of the Royal Society of Chemistry from [28].

concentration, the samples will plot on a hyperbolic line between the two end-members. This hyperbolic curve can be linearized for easier handling by plotting the isotope ratio as a function of the reciprocal Pb concentration (1/[Pb]).

If not two, but three end-members contribute to the final isotope ratios of the samples, the sample data will plot in the three-isotope plot in a triangular field, delimited by lines connecting the ratios of the end-members. As more end-members contribute to the final isotopic signature of a sample, it becomes increasingly more complex to reveal the extent to which the end-members contribute.

**Other Parent–Daughter Pairs** A summary of elements that contain one or more radiogenic nuclides and for which the isotopic composition is studied by (multi-collector) ICP-MS is provided in Table 1.2. Elements with radiogenic nuclides not included in Table 1.2 either are not amenable to ICP-MS analysis (e.g., Ar) or have such long half-lives that the variation in their isotopic compositions is too limited to be quantified using present-day ICP-MS instrumentation.

### 1.4.2
### Effects Caused by Now Extinct Radionuclides

Throughout the history of our solar system, several radionuclides characterized by a half-life that is short with respect to the age of the solar system have become extinct. Variation in the isotopic composition of the element containing the corresponding daughter nuclide is sometimes only noticeable in extra-terrestrial material, such as meteorites. One of these now extinct radionuclides is $^{182}$Hf that $\beta^-$-decayed to $^{182}$Ta with a half-life of $\sim$9 million years. $^{182}$Ta also undergoes $\beta^-$-decay to $^{182}$W with a half-life of only 144 days. As the character of Hf is a lithophile, preferring to reside in the Earth's crust, whereas W is a siderophile, preferring the Earth's core, Hf and W became separated from one another during segregation of the Earth's core. As a result, crustal material has a higher Hf/W elemental ratio than does core material. If differentiation occurred before $^{182}$Hf became extinct, the decay of $^{182}$Hf would have affected the isotopic composition of W in the crust more than if differentiation occurred after $^{182}$Hf became extinct. The Earth's core is not accessible, but iron meteorites can be used as a proxy for planetary cores, including the Earth. Compared with crustal materials on Earth, iron meteorites indeed show lower relative abundances of $^{182}$W. The $^{182}$Hf–$^{182}$W chronometer can therefore be used to constrain the timing of planet differentiation [29].

Another example of an extinct isotope is $^{107}$Pd that $\beta^-$-decayed into $^{107}$Ag with a half-life of 6.5 million years. The $^{107}$Ag/$^{109}$Ag ratio is nearly constant at 1.08 for terrestrial materials, whereas iron meteorites have ratios as high as 9. No terrestrial materials have a Pd/Ag elemental ratio high enough to have resulted in such high $^{107}$Ag/$^{109}$Ag ratios [30, 31].

### 1.4.3
### Mass-Dependent Isotope Fractionation

As a result of their difference in mass, the isotopes of an element can participate in physical processes and/or chemical reactions with slight differences in efficiency,

**Table 1.2** Elements with radiogenic nuclides that can be measured via (multi-collector) ICP-MS [9, 16].

| Element containing radiogenic nuclide(s) | Isotopes (isotopic abundance as mole fraction [11]) with radiogenic nuclides indicated by the arrow | Parent radionuclide ($T_{1/2}$) | Radioactive decay |
|---|---|---|---|
| Sr | $^{84}$Sr (0.0055–0.0058)<br>$^{86}$Sr (0.0975–0.0999)<br>$\Rightarrow$ $^{87}$Sr (0.0694–0.0714)<br>$^{88}$Sr (0.8229–0.8275) | $^{87}$Rb (48.8 $\times$ $10^9$ years) | $^{87}\mathrm{Rb} \rightarrow {}^{87}\mathrm{Sr} + \beta^- + \bar{\nu}$ |
| Nd | $^{142}$Nd (0.2680–0.2730)<br>$\Rightarrow$ $^{143}$Nd (0.1212–0.1232)<br>$^{144}$Nd (0.2379–0.2397)<br>$^{145}$Nd (0.0823–0.0835)<br>$^{146}$Nd (0.1706–0.1735)<br>$^{148}$Nd (0.0566–0.0678)<br>$^{150}$Nd (0.0553–0.0569) | $^{147}$Sm (1.06 $\times$ $10^{11}$ years) | $^{147}\mathrm{Sm} \rightarrow {}^{143}\mathrm{Nd} + \alpha$ |
| Hf | $^{174}$Hf (0.001619–0.001621)<br>$\Rightarrow$ $^{176}$Hf (0.05206–0.05271)<br>$^{177}$Hf (0.18593–0.18606)<br>$^{178}$Hf (0.27278–0.27297)<br>$^{179}$Hf (0.13619–0.13630)<br>$^{180}$Hf (0.35076–0.35100) | $^{176}$Lu (3.57 $\times$ $10^{10}$ years) | $^{176}\mathrm{Lu} \rightarrow {}^{176}\mathrm{Hf} + \beta^- + \bar{\nu}$[a] |
| Os | $^{184}$Os[b]<br>$^{186}$Os<br>$\Rightarrow$ $^{187}$Os<br>$^{188}$Os<br>$^{189}$Os<br>$^{190}$Os<br>$^{192}$Os | $^{187}$Re (4.161 $\times$ $10^{10}$ years) | $^{187}\mathrm{Re} \rightarrow {}^{187}\mathrm{Os} + \beta^- + \bar{\nu}$ |
| Pb | $^{204}$Pb (0.0104–0.0165)<br>$\Rightarrow$ $^{206}$Pb (0.2084–0.2748)<br>$\Rightarrow$ $^{207}$Pb (0.1762–0.2365)<br>$\Rightarrow$ $^{208}$Pb (0.5128–0.5621) | $^{238}$U (4.468 $\times$ $10^9$ years)<br>$^{235}$U (0.407 $\times$ $10^9$ years)<br>$^{232}$Th (14.010 $\times$ $10^9$ years) | See Figure 1.4 |

[a] There is also a smaller fraction (3%) of $^{176}$Lu that decays to $^{176}$Yb via electron capture.
[b] No information provided in [11].

leading to mass-dependent isotope fractionation. In addition to mass-dependent fractionation, mass-independent isotope fractionation has also been observed for metalloids and metallic elements (see below), but their occurrence is much less common and their effect often less substantial. As a result, mass-independent fractionation effects were discovered later and are still less understood. When in a text or scientific paper there is no indication of whether the isotope fractionation is

mass-dependent or mass-independent, it is implicitly assumed to be mass-dependent.

Because the changes in the isotopic composition due to isotope fractionation are small and a difference in isotope ratios relative to one another can be determined more easily than an absolute isotope ratio, an isotope ratio for a sample is usually expressed as the difference between the specific isotope ratio and that of a selected standard:

$$\delta = \frac{R_{\text{sample}} - R_{\text{standard}}}{R_{\text{standard}}} \times 1000(‰)$$

The difference is multiplied by 1000, and thus expressed in units of permil (‰), to obtain values that can be dealt with easily. Because increasingly small differences in isotope ratios can be measured, a multiplication factor of 10 000 is sometimes used (ε values):

$$\varepsilon = \frac{R_{\text{sample}} - R_{\text{standard}}}{R_{\text{standard}}} \times 10\,000$$

Mass-dependent isotope fractionation effects provide insight into the physical processes and chemical reactions during which they occurred and the prevailing conditions (such as pH, temperature, salinity, and oxidation potential). As a result, determination of isotope ratios affected by mass-dependent fractionation in samples that are chronological archives, such as speleothems, corals, or forams, can be used as paleoproxies for the conditions mentioned above, as will be discussed for paleoredox proxies in Chapter 11.

#### 1.4.3.1 Isotope Fractionation in Physical Processes

A very relevant example of mass-dependent isotope fractionation involves the slow evaporation of water out of a glass. The water vapor produced is slightly isotopically lighter than the liquid water remaining in the glass because the phase with the stronger bonds, in this case liquid water, preferentially takes up the heavier isotope. This is because it requires less energy for a water molecule containing the lighter $^{16}O$ to be transferred from the liquid to the gas phase than it does for a water molecule containing $^{18}O$. When the glass is half empty, the remaining water will be slightly enriched in $^{18}O$ compared with the water originally present in the full glass. The variation in the isotopic composition of O remaining in the glass can be described by the Rayleigh equation [32], which describes distillation or condensation under equilibrium conditions:

$$R_t = R_0 f_t^{(\alpha-1)}$$

where $R_t$ is the $^{18}O/^{16}O$ ratio in the liquid phase at time $= t$, $R_0$ the same isotope ratio at time $= 0$, $f_t$ the fraction of water remaining in the glass at time $t$ and $\alpha$ the fractionation factor. In the case of evaporation of liquid water, the fractionation factor $\alpha$ is defined as

$$\alpha = \sqrt{\frac{(^{18}O/^{16}O)_{vapor}}{(^{18}O/^{16}O)_{liquid}}}$$

This fractionation factor varies as a function of temperature, approaching 1 at high temperatures for most processes and reactions.

Rayleigh's law can be applied in a physicochemical process in which the substrate is "consumed" and the product is removed. It is clear that the denser of the two phases considered will become enriched in the heavier of the two isotopes considered.

#### 1.4.3.2 Isotope Fractionation in Chemical Reactions

For metals and metalloids, the isotope fractionation accompanying chemical transformations is of scientific interest. In the late 1940s, the pioneers Bigeleisen and Urey published papers describing the theoretical origin of isotope fractionation effects [33–36] and investigations into the mechanisms of isotope fractionation are still ongoing. Mass-dependent isotope fractionation in chemical reactions is a quantum mechanical phenomenon, into which basic or intuitive insights can be obtained from potential energy curves and vibrational energy levels for the molecules involved in the reaction.

Consider the simple example of the dissociation of a diatomic molecule into the corresponding atoms. The potential energy curve for a diatomic molecule can be approximated as a harmonic oscillator, for which the vibrational energy ($E_{vib}$) is quantized (Figure 1.6) [37, 38]. The molecule vibrates with a specific frequency, and the maximum displacement of the constituent atoms with respect to the

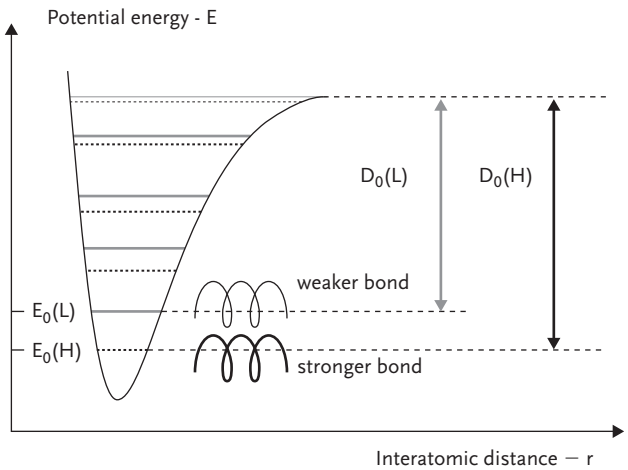


**Figure 1.6** Potential energy as a function of interatomic distance in a diatomic molecule (Morse curve) showing vibrational energy levels for molecules containing the heavier (H) and lighter (L) of the two isotopes considered. The dissociation energies $D_0$ for these two types of molecules are also indicated.
Reproduced with permission of Springer from [37].

center can only adopt specific values. As a result, the diatomic molecule considered can only occupy discrete vibrational energy levels, described by

$$E_{\text{vib}} = \left(n + \frac{1}{2}\right)h\nu$$

where $n$ is the vibrational quantum number, $h$ Planck's constant, and $\nu$ the vibrational frequency, which is determined by the force constant $k$ (corresponding to the bond strength within the molecule) and the reduced mass of the diatomic molecule $\mu$:

$$\nu = \frac{1}{2\pi}\sqrt{\frac{k}{\mu}}$$

The reduced mass is defined as

$$\frac{1}{\mu} = \frac{1}{m_1} + \frac{1}{m_2}$$

or

$$\mu = \frac{m_1 m_2}{m_1 + m_2}$$

where $m_1$ and $m_2$ are the masses of the constituent atoms.

From the above equations, it is clear that a diatomic molecule containing a heavier isotope will show a higher reduced mass than one with a lighter isotope. As a result, the latter will vibrate at a higher frequency. Vibrational energies for molecules containing the heavier and the lighter isotope, respectively, will be shifted with respect to one another.

When external energy such as heat or light is provided to the molecule, its vibrational energy can increase stepwise and ultimately the molecule can dissociate into the constituent atoms. The energy difference between the lowest vibrational energy level (with $n = 0$) and the level at which there is no more attraction between the atoms is termed the dissociation energy, which will differ depending on whether the light or the heavy isotope is present in the molecule. As a result, a molecule containing the light isotope will dissociate more readily than one containing the heavy isotope, resulting in mass-dependent fractionation whereby the molecule will be enriched in the heavier isotope and the separated atoms in the lighter isotope.

For more complex chemical reactions, consider that the reactants interact and form an activated complex, which can then be converted into the reaction products. The corresponding changes in potential energy are depicted for an exothermic reaction (assuming the contribution of the change in entropy $\Delta S$ to be negligible compared with that in enthalpy, such that $\Delta G = \Delta H - T\Delta S \approx \Delta H$) in Figure 1.7. If an element with more than one isotope is present, potential energy curves and vibrational energy levels for each of the stages involved, namely reagent, activated complex, and reaction product, will exist. A distinction can be

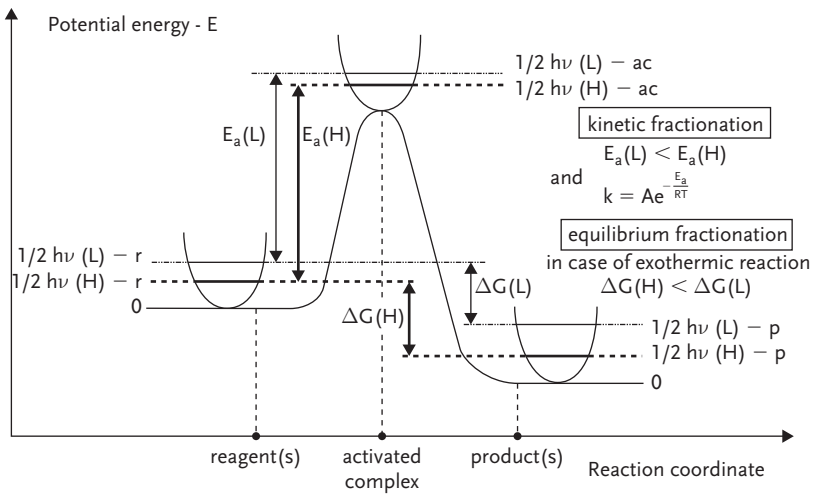


**Figure 1.7** Variation of the potential energy as a function of the reaction coordinate. The potential energy curves for the reagent, activated complex, and reaction product containing the element considered are indicated, together with the vibrational energy levels, which vary according to the mass of the isotope present. Differences in $\Delta G$ govern thermodynamic isotope fractionation, whereas differences in $E_a$ govern kinetic isotope effects. The latter occur when equilibrium cannot be reached.

made between two conditions: (i) one where chemical equilibrium is established and (ii) one where chemical equilibrium is not reached within the time frame considered.

If equilibrium can be established, the fractionation is of thermodynamic origin and its extent is governed by the difference in vibrational energy levels of both reagent and reaction product as a function of isotope mass. $\Delta G$ values differ depending on whether the light or the heavy isotope is present and this affects the equilibrium constant, as:

$$K = e^{-\frac{\Delta G}{RT}}$$

where $R$ is the universal gas constant and $T$ the prevailing temperature. The reagent or reaction product characterized by the strongest chemical bond will be enriched in the heavier isotope.

If within the time frame considered, however, chemical equilibrium is not attained, such as when the reaction is unidirectional (as in enzymatic reactions), when the reaction is proceeding at a relatively low temperature, or when the reaction products are removed, the fractionation is of kinetic origin and its extent is governed by the difference in vibrational energy levels of both reagent and activated complex. Activation energies ($E_a$) differ depending on whether the light or the heavy isotope is present and this affects the reaction rate $k$ according to

$$k = Ae^{-\frac{E_a}{RT}}$$

where $A$ is a constant, characteristic of the reaction considered.

The extent of isotope fractionation can be quantitatively expressed via the fractionation factor α:

$$\alpha = \frac{\left(\frac{N_2}{N_1}\right)_{\text{reaction product}}}{\left(\frac{N_2}{N_1}\right)_{\text{reagent}}} = \frac{\left(\frac{n_2}{n_1}\right)_{\text{reaction product}}}{\left(\frac{n_2}{n_1}\right)_{\text{reagent}}}$$

where $N$ represents the number of nuclides and $n$ the number of moles of the two isotopes considered.

If an element shows three isotopes or more, the mass dependence (usually – see below) of the isotope fractionation observed is expressed by the mass fractionation law:

$$\alpha_2 = \frac{\left(\frac{N_2}{N_1}\right)_{\text{reaction product}}}{\left(\frac{N_2}{N_1}\right)_{\text{reagent}}} \quad \text{and} \quad \alpha_3 = \frac{\left(\frac{N_3}{N_1}\right)_{\text{reaction product}}}{\left(\frac{N_3}{N_1}\right)_{\text{reagent}}}$$

with $\alpha_2 = \alpha_3^{\beta}$. It can be shown [39] that if the isotope fractionation is purely thermodynamically controlled, the mass fractionation factor β corresponds to

$$\beta = \frac{\frac{1}{m_1} - \frac{1}{m_2}}{\frac{1}{m_1} - \frac{1}{m_3}}$$

where $m$ is the atomic mass.

If, on the other hand, the isotope fractionation is kinetically controlled, the mass fractionation factor β corresponds to

$$\beta = \frac{\ln(m_1) - \ln(m_2)}{\ln(m_1) - \ln(m_3)}$$

where $m$ is either the atomic mass or the molecular mass of the compound containing the element under consideration for a transport process or the reduced mass for a process involving breaking bonds.

Maréchal *et al.* [40] defined a generalized law for the mass fractionation factor β:

$$\beta = \frac{m_1^n - m_2^n}{m_1^n - m_2^n}$$

in which $n = -1$ in the case of purely thermodynamic isotope fractionation, and approaches 0 for kinetically governed isotope fractionation.

Calculation of the mass fractionation factor β from experimental data provides insight into whether thermodynamic or equilibrium as opposed to kinetic effects are at the origin of the mass-dependent isotope fractionation, although often the fractionation is shown to be of "mixed" origin. For example, Wombacher *et al.*

studied the evaporation of molten Cd to determine the nature of the isotope fractionation thereby occurring [41]. The data plotted on a three-isotope plot with one isotope ratio of Cd plotted as a function of another one with a common denominator showed a linear relationship. The slope of the best-fitting straight line is the experimental value for β, which was compared with the predicted values based on the assumption of either purely thermodynamic or purely kinetic fractionation. The authors concluded that both kinetically and thermodynamically governed fractionation accompanied the process, resulting in a value of $-0.35$ for the exponent $n$.

The extent to which isotope fractionation is observed for a given element is determined by both the relative mass difference between its isotopes and the extent to which the element participates in physical processes and/or chemical reactions. For the light elements H, C, N, O, and S, variations in their isotopic composition caused by mass-dependent isotope fractionation have been extensively studied using gas source isotope ratio mass spectrometry. For most of the metallic and metalloid elements (except Li and B), the relative mass difference between the isotopes is more limited, such that the variation in isotopic composition thus created is considerably more limited. The high precision with which isotope ratios can be measured nowadays however, not only allows the small isotope fractionations to be revealed, but also quantified. Even for the heaviest naturally occurring element U, variation in its isotopic composition due to the occurrence of isotope fractionation has been demonstrated [13]. As a general rule, elements that can occur in the environment in several oxidation states tend to show more pronounced isotope fractionation.

The introduction of multi-collector ICP-MS has given rise to a breakthrough in this field and the corresponding studies are providing useful information in a variety of fields, as will be illustrated in later chapters. For a more detailed description of isotope fractionation in a variety of processes, the reader is referred to [42].

### 1.4.4
### Mass-Independent Isotope Fractionation

All of the isotope fractionation effects discussed so far are "mass-dependent." This means that there is a linear relationship between the extent of fractionation observed and the mass difference between the isotopes considered. Some processes, however, give rise to an apparently aberrant behavior, whereby one or more isotopes display an additional effect on top of the well-understood mass-dependent fractionation. This apparently aberrant behavior is referred to as "mass-independent" or "anomalous" isotope fractionation. This effect is illustrated in Figure 1.8, where the extent of isotope fractionation experimentally observed for methylation of inorganic Sn using methylcobalamine is plotted as a function of the mass difference between the Sn isotope considered and the reference isotope $^{116}$Sn. When this reaction proceeds in the dark, only mass-dependent fractionation is observed for all isotopes. However, under UV radiation, the two odd-numbered isotopes of Sn studied show a considerably more pronounced fractionation effect

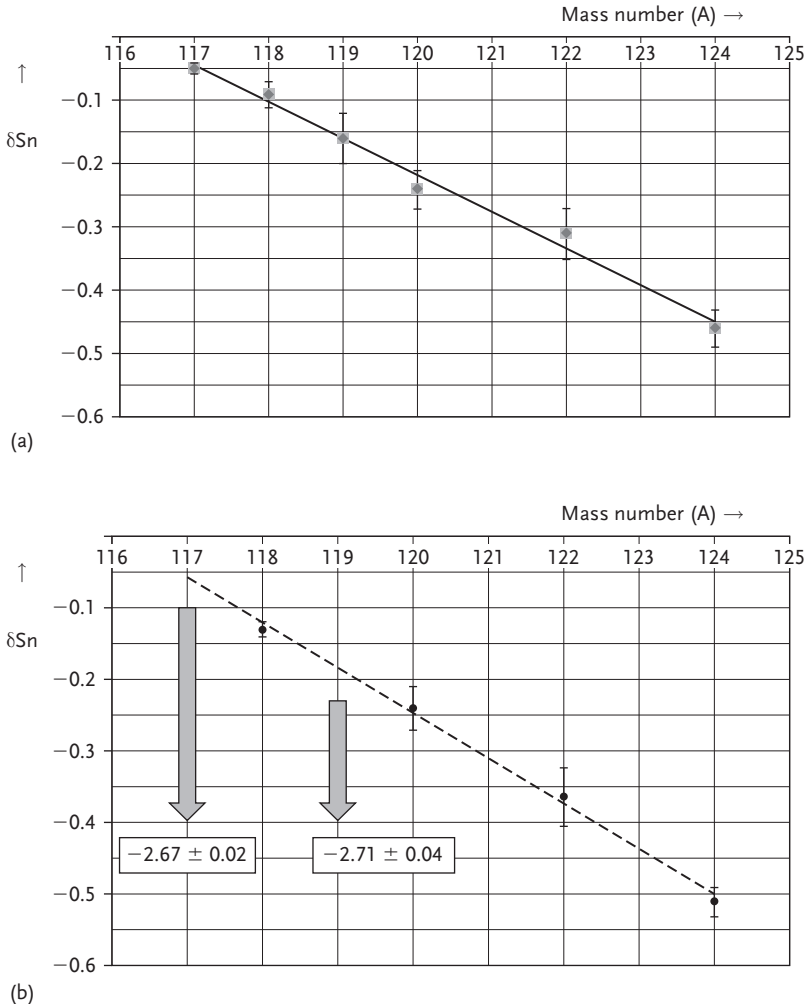


**Figure 1.8** Isotope fractionation, expressed as $\delta_{Sn} = [(^{nnn}Sn/^{116}Sn)_{MeSn}/(^{nnn}Sn/^{116}Sn)_{inorganic\ Sn}] - 1 \times 1000‰$, for methylation of inorganic Sn using methylcobalamine as a function of the mass difference between the isotopes and the reference isotope $^{116}Sn$. (a) Reaction in the dark, wherein only mass-dependent fractionation is observed. (b) Reaction under UV irradiation, which shows mass-independent fractionation for the odd-numbered isotopes $^{117}Sn$ and $^{119}Sn$ in addition to mass-dependent fractionation.
Reproduced with permission of the Royal Society of Chemistry from [43].

and the corresponding results deviate from the linear correlation observed on the basis of the data for the other, even-numbered Sn isotopes. Below, such effects will be consistently termed mass-independent isotope fractionation.

The extent of *mass-independent* fractionation is indicated by the capital delta ($\Delta$) value and is calculated by subtraction of the contribution from mass-dependent fractionation, as estimated from the behavior of the isotopes only displaying

mass-dependent fractionation, from the experimentally observed fractionation [44]. For the example of Sn, the mass-independent contribution is calculated as follows [39, 45]:

$$\Delta^{117}\mathrm{Sn}/^{116}\mathrm{Sn} = \delta^{117}\mathrm{Sn}/^{116}\mathrm{Sn} - \left[\ln\left(\frac{m^{117}\mathrm{Sn}/m^{116}\mathrm{Sn}}{m^{124}\mathrm{Sn}/m^{116}\mathrm{Sn}}\right) \times \delta^{124}\mathrm{Sn}/^{116}\mathrm{Sn}\right]$$

$$\Delta^{118}\mathrm{Sn}/^{116}\mathrm{Sn} = \delta^{118}\mathrm{Sn}/^{116}\mathrm{Sn} - \left[\ln\left(\frac{m^{118}\mathrm{Sn}/m^{116}\mathrm{Sn}}{m^{124}\mathrm{Sn}/m^{116}\mathrm{Sn}}\right) \times \delta^{124}\mathrm{Sn}/^{116}\mathrm{Sn}\right]$$

$$\Delta^{119}\mathrm{Sn}/^{116}\mathrm{Sn} = \delta^{119}\mathrm{Sn}/^{116}\mathrm{Sn} - \left[\ln\left(\frac{m^{119}\mathrm{Sn}/m^{116}\mathrm{Sn}}{m^{124}\mathrm{Sn}/m^{116}\mathrm{Sn}}\right) \times \delta^{124}\mathrm{Sn}/^{116}\mathrm{Sn}\right]$$

$$\Delta^{120}\mathrm{Sn}/^{116}\mathrm{Sn} = \delta^{120}\mathrm{Sn}/^{116}\mathrm{Sn} - \left[\ln\left(\frac{m^{120}\mathrm{Sn}/m^{116}\mathrm{Sn}}{m^{124}\mathrm{Sn}/m^{116}\mathrm{Sn}}\right) \times \delta^{124}\mathrm{Sn}/^{116}\mathrm{Sn}\right]$$

$$\Delta^{122}\mathrm{Sn}/^{116}\mathrm{Sn} = \delta^{122}\mathrm{Sn}/^{116}\mathrm{Sn} - \left[\ln\left(\frac{m^{122}\mathrm{Sn}/m^{116}\mathrm{Sn}}{m^{124}\mathrm{Sn}/m^{116}\mathrm{Sn}}\right) \times \delta^{124}\mathrm{Sn}/^{116}\mathrm{Sn}\right]$$

Only for $^{117}$Sn and $^{119}$Sn and when the reaction proceeds under UV irradiation do the $\Delta$ values differ from zero.

Nuclear volume effects, sometimes referred to as nuclear field shift effects, are believed to be one cause of mass-independent isotope fractionation [46]. Nuclei of isotopes differ from one another only in their number of neutrons. Self-evidently, this provides the isotopes with a different mass, but this may also give rise to differences in the size and shape of the nuclei among the isotopes. The nuclei of nuclides with an odd number of neutrons are often smaller than they should be based on the mass difference relative to those of the neighboring nuclides with an even number of neutrons [47]. These differences in nuclear shape and size, and thus charge density, affect the interaction between the nucleus and the surrounding electron cloud. The resulting difference between the isotopes in terms of density and shape of the electron cloud results in slight differences in the efficiency with which they participate in chemical reactions [48].

The magnetic character of some nuclei also plays an important role in mass-independent fractionation effects. Nuclides characterized by an odd number of protons or odd number of neutrons are characterized by a non-zero nuclear spin. This is what makes these nuclides amenable to investigation by nuclear magnetic resonance (NMR) spectroscopy. A non-zero nuclear spin, however, also affects the interaction between the nucleus and the surrounding electron cloud via hyperfine nuclear spin–electron spin coupling, and thus also the behavior of these nuclides in chemical reactions [49, 50].

The methylation of inorganic Sn using methylcobalamine discussed above showed mass-independent fractionation related to radicals taking part in the reaction under UV irradiation [45, 51]. Conditions leading to a reduced occurrence of radicals, for example the presence of radical scavengers such as particles or $OH^-$ ions, were found to decrease the extent of or even remove the mass-independent fractionation observed for $^{117}$Sn and $^{119}$Sn. Under conditions

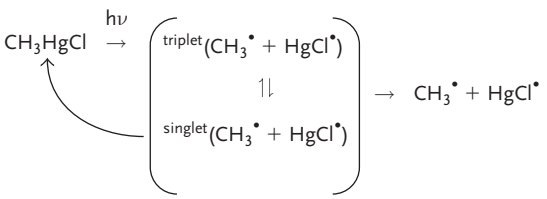


**Figure 1.9** Radicalar reaction process for demethylation of $MeHg^{+}$ under UV radiation. Reproduced with permission of the Royal Society of Chemistry from [51].

favoring the existence of radicals, however, interaction between the nuclear spin of the odd-numbered Sn isotopes and their electron cloud is hypothesized to make these isotopes more amenable for the radicalar reactants, thus leading to an enrichment of the odd-numbered isotopes in methylated Sn.

Another reaction studied by Malinosvky *et al.* is the demethylation of methylmercury MeHgX under UV radiation, another process accompanied by mass-independent fractionation [51]. As shown in Figure 1.9, under the influence of UV radiation, the MeHgCl molecule is split and a short-lived so-called caged radical pair is formed. This caged radical pair is in triplet electron spin state – both electrons show the same electron spin. These radicals can either diffuse away from one another and then the Hg becomes demethylated, or a triplet–singlet electron spin conversion may occur, such that the MeHgCl can be formed again. Owing to hyperfine coupling between nuclear and electron spins, triplet–singlet conversion is believed to proceed faster for the odd-numbered Hg isotopes, so that these become enriched in the methylated form of Hg. Model calculations show that the experimental observations could not be explained solely by nuclear volume effects.

Although currently very much an "academic" topic, the study of mass-independent fractionation of metals and metalloids is also believed to have practical applications. Mass-independent fractionation provides the element with a very specific isotopic signature. For environmentally important elements, such as Hg and Sn, this can be exploited to reveal their sources and understand conversions, thereby enhancing our understanding of their biogeochemical cycles. Such fingerprints have already been demonstrated for Hg in real-life samples [52–54].

Epov *et al.* recently reviewed the literature on mass-independent fractionation for metals and metalloids [55], showing that in this emerging field most of the research so far has been devoted to Hg. However, in addition to Hg, mass-independent fractionation has been reported for Ba, Cd, Cr, Gd, Mo, Nd, Pb, Sm, Sn, Sr, Ru, Te, Ti, Zn, U, and Yb [48, 55].

### 1.4.5
### Interaction of Cosmic Rays with Terrestrial Matter

The best known example of interactions between cosmic rays and terrestrial matter affecting the isotopic composition of an element is the production of $^{14}C$ from $^{14}N$ by (n,p) reactions in the atmosphere. The neutrons involved in the

nuclear reaction are produced by spallation of nuclides in the atmosphere under the influence of cosmic radiation. $^{14}C$, a radionuclide with a half-life of 5730 years, is oxidized to $CO_2$ and enters the food chain via photosynthesis, thus affecting the isotopic composition of C in all living organisms. As long as an organism is alive, the supply and the decay of $^{14}C$ are in dynamic equilibrium and the $^{14}C$ fraction of the carbon present in living organisms is on the order of $10^{-10}$%. Once the organism dies, $^{14}C$ is no longer taken up and the $^{14}C$ present decays. Measurement of the remaining fraction of $^{14}C$ can provide information on the time of death for human or animal remains and materials from plants, such as wood. This forms the basis for radiocarbon or $^{14}C$ dating [15]. For many decades, $^{14}C$ dating has been performed using radiometric techniques, but AMS is now the method of choice because radiometric techniques can only use those $^{14}C$ atoms that decay during the duration of the measurement, whereas AMS can detect each of the $^{14}C$ atoms present [56–59].

Although the cosmic radiation is predominantly absorbed in the atmosphere, a small fraction reaches the surface of the Earth and both stable and radioactive cosmogenic nuclides can be produced. Owing to the very long half-lives of some of the radionuclides produced, such as $^{10}Be$ ($\sim 1.6 \times 10^6$ years) and $^{26}Al$ ($\sim 720 \times 10^3$ years), which are much longer than the half-life of $^{14}C$, radiometric detection is not possible. Because of high sensitivity and minimal spectral interferences, AMS can be used to measure the corresponding isotope ratios, despite their extreme values (e.g., $< 10^{-12}$). Based on knowledge of the production and decay rates of such cosmogenic radionuclides and determination of the corresponding isotope ratios, the duration of surface exposure to cosmic rays can be deduced.

Determination of the extreme isotope ratios encountered in this context is beyond the capabilities of ICP-MS techniques. However, multi-collector ICP-MS has also proven its utility in this context as it was used to obtain a more accurate value for the decay rate of $^{10}Be$ [60]. The radioactivity of a 100 mg $l^{-1}$ solution with a $^{10}Be/^{9}Be$ ratio of $\sim 1.4$ (natural Be is monoisotopic) was measured using liquid scintillation counting, and the $^{10}Be/^{9}Be$ ratio was accurately determined via multi-collector ICP-MS. The combined results provided a half-life of $(1.388 \pm 0.018) \times 10^6$ years, permitting more accurate AMS-based data to be obtained.

### 1.4.6
### Human-Made Variations

The best known example of human-made variations in the isotopic composition of a metal is that of U enrichment. Almost all natural uranium has (nearly) the same isotopic composition, with 99.27% $^{238}U$, 0.72% $^{235}U$, and 0.006% $^{234}U$. The Oklo natural reactor [61] located in Gabon is the only known natural U deposit that shows a significantly different isotopic composition. Because of the earlier occurrence of a natural and self-sustaining fission process, the current relative abundance of $^{235}U$ has become significantly lower than 0.720% at Oklo. A fraction of the $^{235}U$ has been "consumed" during the fission process, as is the case in nuclear fission reactors used to produce energy. This natural fission process could

take place because at the time it occurred (~2 billion years ago), the fraction of $^{235}U$ was high enough to sustain the fission reaction over thousands of years. Evidence of fission in U deposits with much higher grades than Oklo but having ages about 300–400 million years younger has been sought, but was never found.

For energy production in a light-water nuclear plant or for nuclear weapons, the fraction of $^{235}U$ in natural uranium is too low. Therefore, several approaches have been developed to increase the relative abundance of this isotope. For the production of the first atomic bomb at Oak Ridge, TN (USA), $^{235}U$ and $^{238}U$ were separated from one another by "preparative" mass spectrometry using large magnetic sectors (calutrons) after conversion to $UCl_4$ and electron ionization [62]. Isotope fractionation for $^{235}U$ enrichment is also possible via gaseous diffusion, gas centrifugation, or nozzle separation after conversion of U into $UF_6$ [63]. The level of enrichment required is dependent on the final use. Reactor-grade uranium intended for use as "fuel" in a nuclear fission reactor is often called low-grade uranium as an enrichment to 3–4% of $^{235}U$ is sufficient for this purpose. For the production of nuclear weapons, on the other hand, high-grade uranium with an isotopic abundance of $^{235}U \geq 90\%$ is used.

When enriched uranium is produced, depleted uranium (DU) with a $^{235}U$ isotopic abundance of $< 0.720\%$ is also produced as a "waste product." DU is used in the manufacture of ammunition and projectiles that are capable of penetrating armored steel because of the high density of U metal [64]. Upon impact of such projectiles, the temperature rises due to friction and causes the uranium to catch fire and burn. Their use in recent wars in the Middle East and the former Yugoslavia has raised considerable concern because of the chemical toxicity of uranium [65]. DU is also used for the manufacture of counterweights located in the tail and the wings of airplanes with the purpose of increasing stability. The advantage of using DU in this context lies again in its very high density, enabling these counterweights to be compact, thus leaving more space for fuel. Isotopic analysis of U is carried out for a multitude of purposes. Applications based on U isotope ratio measurements are discussed in Chapter 15.

As a result of the industrial use of U, commercially acquired U-containing chemicals or U standard solutions intended for elemental assay purposes will not necessarily have the natural isotopic composition, but will most often be depleted in $^{235}U$ [66]. An unnatural isotopic composition may also be encountered for Li in chemicals, as it may be depleted in $^{6}Li$, as a result of its use as $^{6}LiD$ as fusion fuel in thermonuclear weapons and in nuclear fusion [67].

Another example of an element for which human intervention is required to modify the isotopic composition, thus rendering the element more useful in specific applications, is boron. Natural B is composed of roughly 20% $^{10}B$ and 80% $^{11}B$. As $^{10}B$ shows a thermal neutron cross-section (the probability that it will capture a thermal neutron) that is almost six orders of magnitude higher than that of $^{11}B$, $^{10}B$-enriched boron is used to control the chain reaction in nuclear fission reactors [68]. This enrichment requires human intervention. Upon neutron capture, $^{10}B$ undergoes (n,$\alpha$) reaction, thus producing $^{7}Li$. The production of these short-range $\alpha$-particles also forms the basis for the use of $^{10}B$ in an experimental

anti-cancer therapy, boron neutron capture therapy or BNCT [69]. In BNCT, the patient is first administered a $^{10}$B-containing drug that selectively accumulates in the tumor tissue. Upon radiation with thermal neutrons, the nuclear reaction mentioned above occurs predominantly in tumor cells. The α-particles emitted typically travel a distance of only one cell, thus creating a far higher level of cell destruction for the neoplastic tissue than for the surrounding healthy tissue.

Finally, in the context of elemental assay via isotope dilution and tracer experiments using stable isotopes, an isotopically enriched spike or tracer is added to a sample wherein the element of interest typically shows the natural isotopic composition. These isotopically enriched spikes are another example of human-made variations.

## References


1 Rutherford, E. (1911) The scattering of α and β particles by matter and the structure of the atom. *Philos. Mag.*, **21**, 669–688.

2 Geiger, H. and Marsden, E. (1909) On a diffuse reflection of the alpha-particles. *Proc. R. Soc. Lond. A*, **82**, 495–500.

3 Bohr, N. (1921) Atomic structure. *Nature*, **106**, 104–107.

4 Cunninghame, J.G. (1964) *Introduction to the Atomic Nucleus*, Elsevier, Amsterdam.

5 Budzikiewicz, H. and Grigsby, R.D. (2006) Mass spectrometry and isotopes: a century of research and discussion. *Mass. Spectrom. Rev.*, **25**, 146–157.

6 Thomson, J.J. (1913) Rays of positive electricity. *Proc. R. Soc. Lond. A*, **89**, 1–20.

7 Aston, F.W., The mass-spectra of chemical elements. *Philos. Mag.*, **39**, 611–625.

8 Ehmann, W.D. and Vance, D.E. (1991) *Radiochemistry and Nuclear Methods of Analysis*, John Wiley & Sons, Ltd., Chichester.

9 Faure, G. and Mensing, T.M. (2005) *Isotopes – Principles and Applications*, 3rd edn., John Wiley & Sons, Ltd., Chichester.

10 Lodders, K. (2003) Solar system abundances and condensation temperatures of the elements. *Astrophys. J.*, **591**, 1220–1247.

11 Böhlke, J.K., de Laeter, J.R., De Bièvre, P., Hidaka, H., Peiser, H.S., Rosman, K.J.R., and Taylor, P.D.P. (2005) Isotopic compositions of the elements, 2001. *J. Phys. Ref. Data.*, **34**, 57–67.

12 Faure, G. and Mensing, T.M. (2007) *Introduction to Planetary Science – the Geological Perspective*, Springer, Berlin.

13 Weyer, S., Anbar, A.D., Gerdes, A., Gordon, G.W., Algeo, T.J., and Boyle, E.A. (2008) Natural fractionation of $^{238}$U/$^{235}$U. *Earth Planet. Sci. Lett.*, **72**, 345–359.

14 Navrátil, O., Hàla, J., Kopunec, R., Macásek, F., Mikulaj, V., and Lešetický, L. (1992) *Nuclear Chemistry*, Ellis Horwood, Chichester.

15 Taylor, R.E. (2000) Fifty years of radiocarbon dating. *Am. Sci.*, **88**, 60–67.

16 Dickin, A.P. (2005) *Radiogenic Isotope Geology*, 2nd edn., Cambridge University Press, Cambridge.

17 Balcaen, L., Moens, L., and Vanhaecke, F. (2010) Determination of isotope ratios of metals (and metalloids) by means of ICP-mass spectrometry for provenancing purposes – a review. *Spectrochim. Acta B*, **65**, 769–786.

18 Bourdon, B., Turner, S., Henderson, G.M., and Lundstrom, C.C. (2003) Introduction to U-series geochemistry. *Rev. Miner. Geochem.*, **52**, 1–19.

19 Chow, T.J. and Earl, J.L. (1970) Lead aerosols in the atmosphere: increasing concentrations. *Science*, **169**, 577–580.

20 Ault, W.U., Senechal, R.G., and Erlebach, W.E. (1970) Isotopic composition as a natural tracer of lead

in the environment. *Environ. Sci. Technol.*, **4**, 305–313.
**21** Fachetti, S. (1988) Mass spectrometry applied to studies of lead in the atmosphere. *Mass Spectrom. Rev.*, **7**, 503–533.
**22** Bollhofer, A. and Rosman, K.J.R. (2000) Isotopic source signatures for atmospheric lead: the southern hemisphere. *Geochim. Cosmochim. Acta*, **64**, 3251–3262.
**23** Bollhofer, A. and Rosman, K.J.R. (2001) Isotopic source signatures for atmospheric lead: the northern hemisphere. *Geochim. Cosmochim. Acta*, **65**, 1727–1740.
**24** Moor, H.C., Schaller, T., and Sturm, M. (1996) Recent changes in stable lead isotope ratios in sediments of Lake Zug, Switzerland. *Environ. Sci. Technol.*, **30**, 2928–2933.
**25** Kersten, M., Garbe-Schönberg, D., Thomsen, S., Anagnostou, C., and Sioulas, A. (1997) Source apportionment of Pb pollution in the coastal waters of Elefsis Bay. *Greece Environ. Sci. Technol.*, **31**, 1295–1301.
**26** Vallelonga, P., Gabrielli, P., Balliana, E., Wegner, A., Delmonte, B., Turetta, C., Burton, G., Vanhaecke, F., Rosman, K.J.R., Hong, S., Boutron C.F., Cescon, P., and Barbante, C. (2010) Lead isotopic compositions in the EPICA Dome C ice core and southern hemisphere potential source areas. *Quat. Sci. Rev.*, **29**, 247–255.
**27** Döring, T., Schwikowski, M., and Gaggeler, H.W. (1997) The analysis of lead concentrations and isotope ratios in recent snow samples from high alpine sites with a double focusing ICP-MS. *Fresenius' J. Anal. Chem.*, **359**, 382–384.
**28** Townsend, A.T. and Snape, I. (2002) The use of Pb isotope ratios determined by magnetic sector ICP-MS for tracing Pb pollution in marine sediments near Casey Station, East Antarctica. *J. Anal. At. Spectrom.*, **17**, 922–928.
**29** Jacobsen, S.B. (2005) The Hf–W isotopic system and the origin of the Earth and the Moon. *Annu. Rev. Earth Planet. Sci.*, **33**, 531–570.
**30** Kaiser, T. and Wasserburg, G.J. (1983) The isotopic composition and concentration of Ag in iron meteorites and the origin of exotic silver. *Geochim. Cosmochim. Acta*, **47**, 43–58.
**31** Chen, J.H. and Wasserburg, G.J. (1990) The isotopic composition of Ag in meteorites and the presence of $^{107}$Pd in protoplanets. *Geochim. Cosmochim. Acta*, **54**, 1729–1743.
**32** Rayleigh, W.S. (1896) Theoretical considerations respecting the separation of gases by diffusion and similar processes. *Philos. Mag.*, **42**, 493–498.
**33** Bigeleisen, J. and Mayer, M.G. (1947) Calculation of equilibrium constants for isotopic exchange reactions. *J. Chem. Phys.*, **15**, 261–267.
**34** Urey, H.C. (1947) The thermodynamic properties of isotopic substances. *J. Chem. Soc.*, 562–581.
**35** Bigeleisen, J. (1949) The relative reaction velocities of isotopic molecules. *J. Chem. Phys.*, **17**, 675–678.
**36** Bigeleisen, J. (1965) Chemistry of isotopes. *Science*, **147**, 463–471.
**37** Hoefs, J. (2004) *Stable Isotope Geochemistry*, 5th edn., Springer, Berlin.
**38** Zeebe, R.E. and Wolf-Glabrow, D. (2001) *$CO_2$ in Seawater: Equilibrium, Kinetics, Isotopes*, Elsevier, Amsterdam.
**39** Young, E.D., Galy, A., and Nagahara, H. (2002) Kinetic and equilibrium mass-dependent isotope fractionation laws in Nature and their geochemical and cosmochemical significance. *Geochim. Cosmochim. Acta*, **66**, 1095–1104.
**40** Maréchal, C.N., Telouk, P., and Albarède, F. (1999) Precise isotopic analysis of copper and zinc isotopic compositions by plasma-source mass spectrometry. *Chem. Geol.*, **156**, 251–273.
**41** Wombacher, F., Rehkämper, M., and Mezger, K. (2004) Determination of the mass-dependence of cadmium isotope fractionation during evaporation. *Geochim. Cosmochim. Acta*, **68**, 2349–2357.
**42** Wolfsberg, M., Van Hook, W.A., Paneth, P., and Rebelo, L.P.N. (2010) *Isotope Effects in the Chemical, Geological and Biosciences*, Springer, Berin.

**43** Jakubowski, N., Prohaska, T., Vanhaecke, F., Roos, P.H., and Lindemann, T. (2011) Inductively coupled plasma- and glow discharge plasma-sector field mass spectrometry – Part II: applications. *J. Anal. At. Spectrom.*, **26**, 727–757.

**44** Blum, J.D. and Bergquist, B.A. (2007) Reporting of variations in the natural isotopic composition of mercury. *Anal. Bioanal. Chem.*, **388**, 333–359.

**45** Malinovsky, D., Moens, L., and Vanhaecke, F. (2009) Isotopic fractionation of Sn during methylation and demethylation reactions in aqueous solutions. *Environ. Sci. Technol.*, **43**, 4399–4404.

**46** Bigeleisen, J. (1996) Nuclear size and shape effects in chemical reactions. Isotope chemistry of the heavy elements. *J. Am. Chem. Soc.*, **118**, 3676–3680.

**47** Aufmuth, P., Heilig, K., and Steudel, A. (1987) Changes in mean-square nuclear charge radii from optical isotope shifts. *At. Data Nucl. Data Tables*, **7**, 455–490.

**48** Fujii, T., Moynier, F., and Albarède, F. (2009) The nuclear field shift effect in chemical exchange reactions. *Chem. Geol.*, **267**, 139–158.

**49** Buchachenko, A.L. (1995) MIE versus CIE: comparative analysis of magnetic and classical isotope effects. *Chem. Rev.*, **95**, 2507–2528.

**50** Buchachenko, A.L. (2001) Magnetic isotope effect: nuclear spin control of chemical reactions. *J. Phys. Chem. A*, **105**, 9995–10011.

**51** Malinovsky, D., Latruwe, K., Moens, L., and Vanhaecke, F. (2010) Experimental study of mass-independence of Hg isotope fractionation during photodecomposition of dissolved methylmercury. *J. Anal. At. Spectrom.*, **25**, 950–956.

**52** Laffont, L., Sonke, J.E., Maurice, L., Hintelmann, H., Pouilly, M., Bacarreza, Y.S., Perez, T., and Behra, P. (2009) Mercury isotopic compositions of fish and human hair in the Bolivian Amazon. *Environ. Sci. Technol.*, **43**, 8985–8990.

**53** Gantner, N., Hintelmann, H., Zheng, W., and Muir, D.C. (2009) Variations in stable isotope fractionation of Hg in food webs of Arctic lakes. *Environ. Sci. Technol.*, **43**, 9148–9154.

**54** Feng, X.B., Foucher, D., Hintelmann, H., Yan, Y.H., He, T.R., and Qiu, G.L. (2010) Tracing mercury contamination sources in sediments using mercury isotope compositions. *Environ. Sci. Technol.*, **44**, 3363–3368.

**55** Epov, V.N., Malinovsky, D., Sonke, J.E., Vanhaecke, F., Begue, D., and Donard, O.F.X. (2011) Modern mass spectrometry for studying mass-independent fractionation of heavy stable isotopes in environmental and biological sciences. *J. Anal. At. Spectrom.*, **26**, 1142–1156.

**56** Elmore, D. and Phillips, F.M. (1987) Acclerator mass spectrometry for measurement of long-lived radioisotopes. *Science*, **236**, 543–550.

**57** Vogel, J.S., Turteltaub, K.W., Finkel, R., and Nelson, D.E. (1995) Accelerator mass spectrometry: isotope quantification at attomole sensitivity. *Anal. Chem.*, **67**, 353A–359A.

**58** Filfield, L.K. (1999) Accelerator mass spectrometry and its applications. *Rep. Prog. Phys.*, **62**, 1223–1274.

**59** Helborg, R. and Skog, G. (2008) Accelerator mass spectrometry. *Mass Spectrom. Rev.*, **27**, 398–427.

**60** Chmeleff, J., von Blanckenburg, F., Kossert, K., and Jakob, D. (2010) Determination of the $^{10}$Be half-life by multicollector ICP-MS and liquid scintillation counting. *Nucl. Instrum. Methods B*, **268**, 192–199.

**61** West, R. (1976) Natural nuclear reactors – the Oklo phenomenon. *J. Chem. Educ.*, **53**, 336–340.

**62** Yergey, A.L. and Yergey, A.K. (1997) A brief history of the calutron. *J. Am. Soc. Mass Spectrom.*, **8**, 943–953.

**63** Settle, F.A. (2009) Uranium to electricity: the chemistry of the nuclear fuel cycle. *J. Chem. Educ.*, **86**, 316–323.

**64** Bleise, A., Danesi, P.R., and Burkart, W. (2003) Properties, use and health effects of depleted uranium (DU): a general overview. *J. Environ. Radioact.*, **64**, 93–112.

**65** Priest, N.D. (2001) Toxicity of depleted uranium. *Lancet*, **357**, 244–246.

**66** Richter, S., Alonso, A., Wellum, R., and Taylor, P.D.P. (1999) The isotopic composition of commercially available uranium chemical reagents. *J. Anal. At. Spectrom.*, **14**, 889–891.

**67** Qi, H.P., Coplen, T.B., Wang, Q.Z., and Wang, Y.H. (1997) Unnatural isotopic composition of lithium reagents. *Anal. Chem.*, **69**, 4076–4078.

**68** Choppin, G.R. and Rydberg, J. (1980) *Nuclear Chemistry – Theory and Applications*, Pergamon Press, Oxford.

**69** Barth, R.F., Coderre, J.A., Vicente, M.G.H., and Blue, T.E. (2005) Boron neutron capture therapy of cancer: current status and future prospects. *Clin. Cancer Res.*, **11**, 3987–4002.